

Article

Improved Algorithm for Efficient Extraction of Relaxation Parameter Values from Wideband Permittivity of Baijiu

Haoyan Yu¹, Qi Jin¹, Zhaozong Meng² and Zhen Li^{1,*}

¹ College of Automation Engineering, Nanjing University of Aeronautics and Astronautics, Nanjing 211106, China

² School of Mechanical Engineering, Hebei University of Technology, Tianjin 300401, China

* Corresponding author email: zhenli@nuaa.edu.cn

Abstract: The complex permittivity of baijiu varies with frequency, and dielectric spectroscopy has been used to evaluate the quality. To simplify the analysis and reduce the number of the parameters, a dielectric relaxation model is often used to fit the permittivity data. However, existing fitting methods such as the least squares and particle swarm optimization methods are often computationally complex and require preset initial values. Therefore, a simpler calculation method of the relaxation parameters considering the geometric characteristics of the permittivity spectrum is proposed. It is based on the relationship between the Cole-Cole relaxation parameters and the Cole-Cole diagram, which is fitted by a geometric method. First, the concepts of the Cole-Cole parameters and the diagram are introduced, and then the process of obtaining the parameters from the complex permittivity measurement data is explained. Taking baijiu with 56% alcohol by volume (ABV) as an example, the fitting is better than the least squares method and similar to the particle swarm optimization. This method is then used for the parameter fitting of baijiu with ABV of 42-52%, and the average error is less than 1%, demonstrating its wider applicability. Finally, a prediction model is used for baijiu with 53% ABV, and the error is only 1.51%. Hence, the method can be applied to the measurement of ABV of baijiu.

Keywords: permittivity; cole-cole equation; relaxation parameters; alcohol by volume; baijiu



Copyright: © 2024 by the authors. This article is licensed under a Creative Commons Attribution 4.0 International License (CC BY) license (<https://creativecommons.org/licenses/by/4.0/>).

Citation: Haoyan Yu, Qi Jin, Zhaozong Meng and Zhen Li. "Improved Algorithm for Efficient Extraction of Relaxation Parameter Values from Wideband Permittivity of Baijiu." *Instrumentation* 11, no. 1 (March 2024). <https://doi.org/10.15878/j.instr.202300156>

0 Introduction

Baijiu is a kind of distilled spirit made of grains as the main raw material. It is one of the most consumed alcoholic drinks globally. The concentration of ethanol contained in baijiu is usually expressed in volume fraction, i.e., alcohol by volume (ABV). The ABV of baijiu is 38-65%. In recent years, baijiu fraud incidents have occurred from time to time. They are mainly divided into two categories, mixing of water into the original wine^[1] and blending of industrial alcohol containing toxic impurities such as methanol^[2]. They harm consumer rights and physical health. Hence, the quality inspection of baijiu holds significant importance. There are many methods for its quality detection, such as gas chromatography^[3-5], mass spectrometry^[6], and near-infrared

spectrum^[7,8]. They are generally expensive, requiring samples to be sent to a specialized laboratory for testing, and are not suitable for on-site measurements.

In recent years, microwave technology has been widely used in food quality detection, due to the advantages of low cost, simple experimental setup, high speed, and low signal power. Microwave is an electromagnetic wave with a frequency in the range of 300 MHz-300 GHz. It can obtain information about the sample by measuring the complex permittivity. The main measurement methods include the resonance method^[9,10], transmission line method^[11], coaxial method probe technology, etc. The resonance method obtains the electromagnetic parameters of the sample through the change of the resonance frequency and quality factor. But the parameters at a single frequency are sometimes

difficult to describe all the characteristics. The transmission line method has the limitation of the frequency range. The coaxial probe technology has wider frequencies. Therefore, the coaxial probe technique can be used to obtain the complex permittivity of the sample in a wide frequency band, the dielectric spectrum.

In recent years, dielectric spectrum has been widely used in food-related detection, including the detection of soluble solids content and maturity of fruits^[12,13], the detection of components and freshness of meat, aquatic products and dairy products^[14-17] and online monitoring in the preparation process^[18], edible oil quality detection and evaluation^[19], etc. Dielectric spectrum technology can also be applied to the quality inspection of alcoholic drinks (such as whisky, Fenjiu, baijiu, etc.). For example, Li et al.^[20] measured the complex permittivity of a mixture of ethanol and water at concentrations ranging from 0% to 100% at 10% intervals, covering the frequency range of 200 MHz to 40 GHz. They obtained the dielectric spectrum and proposed a method to distinguish mixtures with a 2% ABV difference based on this data. At the same time, compared with the dielectric properties of Fenjiu with an ABV of 42–62%, it was found that a small amount of other compounds in Fenjiu had no significant effect on the dielectric properties of alcohol. Miura et al.^[21] measured the properties of whiskey with an ABV of 36% in the frequency range of 5–20 GHz. By measuring the properties of whiskey, water and ethanol mixtures in this frequency range, the dielectric constant was found to change with the time the whisky was stored.

The complex permittivity varies with frequency. It can be simplified through mathematical models, and the parameters of the model can be used for the quality analysis of baijiu. The classic complex permittivity models include Debye and Cole-Cole equations. The former is suitable for the description of the complex permittivity of water, while the latter is an extension of the former, describing polarization processes with relaxation time distributions. The latter is suitable for more liquids, such as alcoholic drinks with higher ABV. Therefore, how to fit the parameters by the measured complex permittivity is very important. Bohigas et al.^[22] studied the dielectric properties of 40% ethanol aqueous solution in the frequency range of 1–20 GHz, and obtained Debye parameters of water and several wines with ABV of 0–36% (beer, whiskey, brandy, etc.) by the method of least squares fitting. They were found to be linearly related to ethanol concentration, and the linear model of Debye parameters was given. Li et al.^[23] measured the complex permittivity of baijiu with ABV ranging of 42–56% in the frequency range of 2–20 GHz, and obtained the Cole-Cole parameters of baijiu by particle swarm optimization. It was found that the real and imaginary parts of the complex permittivity and the Cole-Cole parameters are all linearly related to the ABV of baijiu. Both the least squares method and the particle swarm

optimization use an iterative method to find the parameter combining with the highest degree of fitting. The disadvantage of them is that the initial value and range of the parameters usually need to be preset by experience in advance, and they may fall into the problem of local minimum value. A geometric method is proposed for solving parameters based on Cole-Cole diagram features and Cole-Cole equation. Firstly, the Cole-Cole diagram is fitted by geometric relationship, and the parameter value is obtained from the relationship between it and Cole-Cole parameters. Secondly, the complex permittivity of baijiu of 48–56% ABV was fitted, and the ABV measurement model was established. Finally, the scope and calculation process are discussed. The advantage of this method lies in its simplicity in the calculation process. Unlike the iterative method, it does not require the pre-setting of parameters.

1 Materials and Methods

1.1 Calculation of Parameters from the Cole-Cole Equation

The permittivity is a complex number at high frequencies, and its value can be expressed by the Cole-Cole equation, as shown in equation (1):

$$\varepsilon_r = \varepsilon'_r - j\varepsilon''_r = \varepsilon_{r\infty} + \frac{\varepsilon_{r0} - \varepsilon_{r\infty}}{1 + (j\omega\tau)^{1-\alpha}} \quad (1)$$

where ω is the angular frequency, the unit is rad/s; ε_{r0} , $\varepsilon_{r\infty}$ are the limit value of the permittivity at very low and high frequency; τ is the relaxation time, the unit is s; α is the relaxation time distribution parameter. They are real numbers. When $\alpha=0$, it is the Debye equation. The real and imaginary parts of ε_{r0} can be obtained from the Cole-Cole equation, as shown in equations (2) and (3):

$$\varepsilon'_r = \varepsilon_{r\infty} + \frac{(\varepsilon_{r0} - \varepsilon_{r\infty})[1 + (\omega\tau)^{1-\alpha} \sin \frac{\pi}{2} \alpha]}{1 + 2(\omega\tau)^{1-\alpha} \sin \frac{\pi}{2} \alpha + (\omega\tau)^{2-2\alpha}} \quad (2)$$

$$\varepsilon''_r = \frac{(\varepsilon_{r0} - \varepsilon_{r\infty})(\omega\tau)^{1-\alpha} \cos \frac{\pi}{2} \alpha}{1 + 2(\omega\tau)^{1-\alpha} \sin \frac{\pi}{2} \alpha + (\omega\tau)^{2-2\alpha}} \quad (3)$$

On the complex plane, the curve formed by the values of the real and imaginary parts of the complex permittivity is part of a circle, and its intersections with the real axis are ε_{r0} and $\varepsilon_{r\infty}$, as shown in Fig.1. When $\alpha=0$, the part above the real axis is a semicircle. The imaginary part of the complex permittivity can be written in the following form, as shown in equation (4):

$$\varepsilon''_r = \frac{(\varepsilon_{r0} - \varepsilon_{r\infty}) \cos \frac{\pi}{2} \alpha}{\frac{1}{(\omega\tau)^{1-\alpha}} + (\omega\tau)^{1-\alpha} + 2 \sin \frac{\pi}{2} \alpha} \quad (4)$$

When $\omega\tau=1$, its maximum value is shown in equation (5):

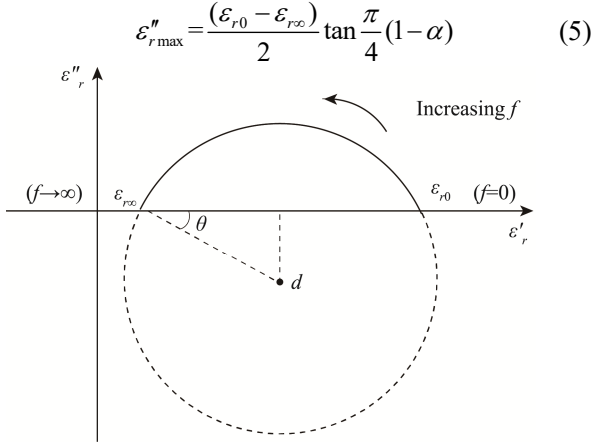


Fig.1 Relationship between the Cole-Cole diagram and relaxation parameters

Taking the radius of the circle as R , the angle between the straight line determined by the intersection of the circle and the real axis and the center of the circle and the real axis as θ , and the distance from the center of the circle to the real axis as d , equations (6)-(8) can be obtained:

$$\theta = \frac{\pi}{2} \alpha \quad (6)$$

$$d = \frac{\varepsilon_{r0} - \varepsilon_{r\infty}}{2} \tan \theta \quad (7)$$

$$R = \frac{\varepsilon_{r0} - \varepsilon_{r\infty}}{2} \cdot [\cos(\frac{\pi}{2} \alpha)]^{-1} \quad (8)$$

1.2 Calculation of Cole-Cole Parameters from Complex Permittivity Measurements

If the complex permittivity at three frequency points is measured, the center of the circle can be obtained by calculating the intersection of the vertical bisectors through geometric relations. The equation of the circle and its intersections with the real axis ε_{r0} , $\varepsilon_{r\infty}$ can be obtained. Then, θ can be obtained from the distance d from the center of the circle to the real axis, and α can be obtained according to equation (6). Finally, the obtained three parameters are brought into the Cole-Cole equation, and the two values of $\omega\tau$ can be obtained. After judging the frequency according to ε_{r0} , the τ value can be obtained.

1.3 Frequency Point Selection

The Cole-Cole parameter can be calculated from a set of measured values of complex permittivity at three different frequencies, but there are often errors. In this case, multiple sets of measured values are needed to fit the parameter values. However, the measured frequency range contains multiple data, and the selection of frequency points has a greater impact on the results at this time. If the frequency points are too close, the equation of the Cole-Cole circle calculated from the frequency points may have large errors. So three frequency points are selected by the method of equal real axis spacing, and the spacing is one-third of the maximum difference of the real

part of the data, as shown in Fig.2. m is the maximum difference of the real part of the data, and 50 points are taken. The initial point n of each time is a random number in the range of 0 to $m/3$. The final result is averaged. The error δ is used as the evaluation index, as shown in equation (9):

$$\delta = \frac{1}{N_f} \sum_{i=1}^{N_f} \left| \frac{\varepsilon_{ri} - \hat{\varepsilon}_{ri}}{\varepsilon_{ri}} \right| \quad (9)$$

where N_f is the number of frequency points; ε_{ri} is the measured value of the complex permittivity; $\hat{\varepsilon}_{ri}$ is the complex permittivity obtained by inverse calculation of the parameters.

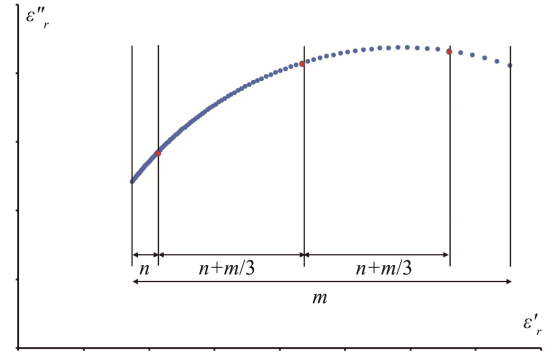


Fig.2 Schematic diagram of the isometric axis method

1.4 Experimental Setup

The complex permittivity of baijiu was measured by the coaxial probe method, and the experimental setup is shown in Fig.3. A coaxial probe is connected to the FieldFox N9951A portable microwave analyzer through an SMA connector and a coaxial cable. The analyzer is connected to a computer by a LAN cable, and the computer sends commands to the analyzer through SCPI for measurement. Data acquisition and processing were conducted using MATLAB 2014a software, developed by MathWorks, on the computer. The room temperature is 20 °C, and the frequency range is from 3 to 20 GHz. The signal power was set to 0.032 W to avoid thermal effects. The IF bandwidth was chosen to be 100 Hz to reduce noise effects. The ABV of baijiu is respectively 42%, 45%, 50%, 52%, 53% and 56%. The probe is secured to the laboratory table, baijiu is poured into the beaker, and it is then placed on the lifting platform. The height is adjusted to position the probe 12 mm below the liquid surface. Each set of data was measured three times, and the probe was washed with distilled water and wiped dry after each measurement. Standard ethanol and distilled water were measured at the same time, and the complex permittivity of baijiu was calculated by the error correction method^[23]. Fig.4 shows the complex permittivity data of baijiu with different ABV.

2 Results and Analysis

2.1 Calculation Method Verification

The standard complex permittivity data of water

were first fitted to verify the feasibility of the method. The Cole-Cole parameters^[24] ($\epsilon_{r0}=80.35$, $\epsilon_{r\infty}=4.23$, $\tau=9.31$ ps, $\alpha=0.013$) of water at 20°C are brought into the Cole-Cole equation within 2-20 GHz. The ideal complex permittivity of water is obtained by taking 300 frequency points at equal intervals within 2-20 GHz. The parameters

are fitted by geometric method. The results are completely consistent with the parameters taken, and the error is exceedingly small and can be practically disregarded. The fitting effect is shown in Fig.5. The Cole-Cole parameter obtained by this method has no error. The method is feasible.

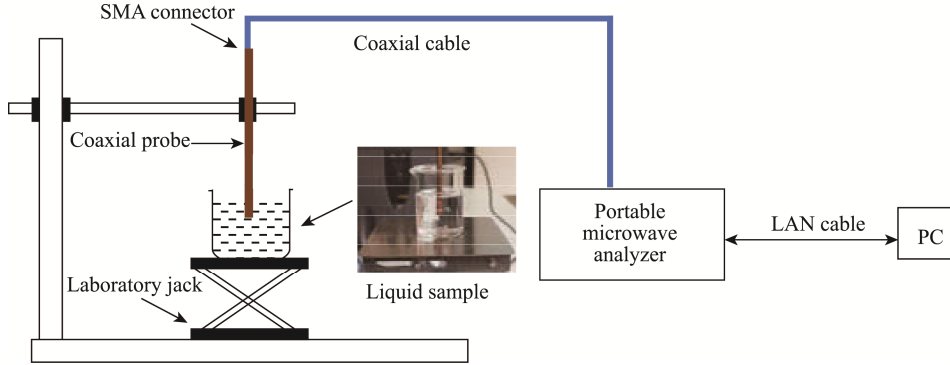


Fig.3 Experimental setup for measuring permittivity of baijiu by coaxial probe method

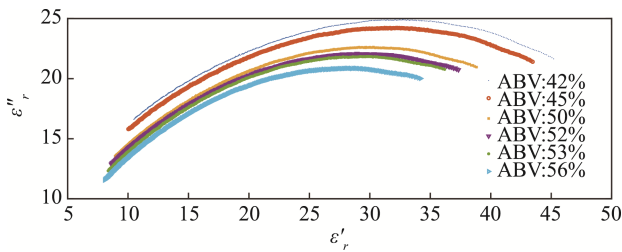


Fig.4 Complex permittivity values of baijiu samples measured

2.2 Cole-Cole Parameter Fitting of baijiu

First, taking baijiu with an ABV of 56% as an example, the geometrical method was used to fit the complex permittivity data of 3-20 GHz. The results are shown in Table 2. At the same time, it is compared with the nonlinear least squares method (the result is calculated

by the lsqnonlin function in Matlab) and the particle swarm optimization. The Cole-Cole circles fitted by the three methods are shown in Fig.6. For 56% baijiu, the least squares method has a poor fitting effect on the complex permittivity at low frequencies, resulting in the shift of the

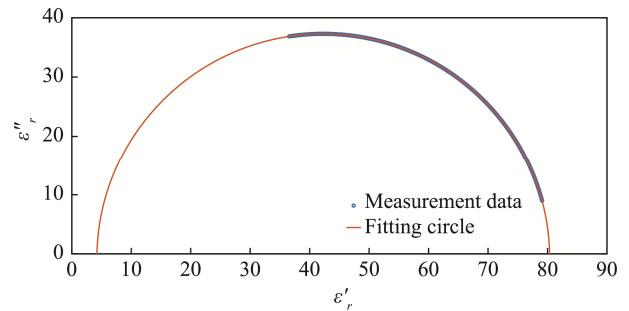


Fig.5 Complex permittivity of water and fitting Cole-Cole diagram

Table 1 Parameters of baijiu of 56% ABV fitting with three methods

Method	ϵ_{r0}	$\epsilon_{r\infty}$	α	τ /ps	δ /%
Geometric method	54.45±0.56	2.77±0.26	0.13±0.01	36.27±0.49	0.68
Least squares method	48.40	3.34	0.07	30.0	1.79
Particle swarm optimization	53.19	2.65	0.13	34.79	0.59

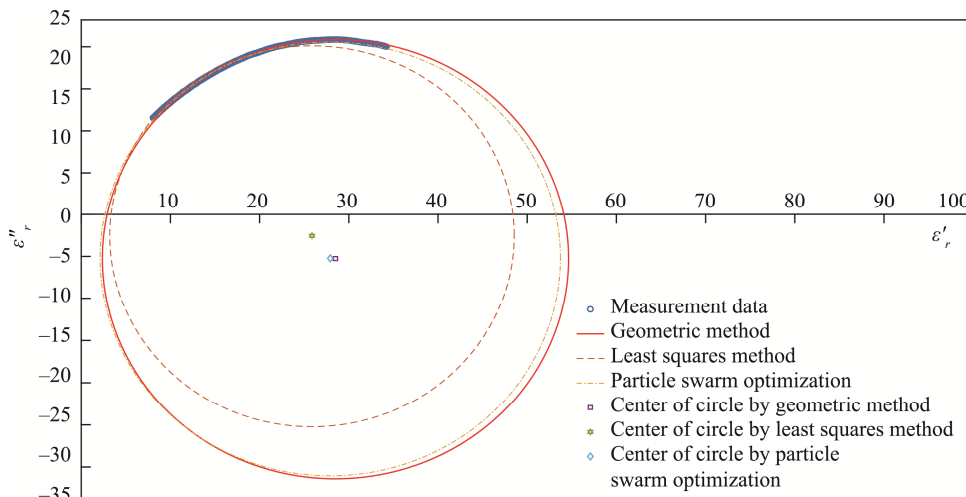


Fig.6 Comparison of the circles fitting by three fitting methods

center of the circle. The fitting circle has a small radius. While the geometric method and the particle swarm optimization have a better fitting effect on the data, the δ value obtained by them is no more than 1%, and the error of the Cole-Cole parameters is small.

The fitting results of the parameters for baijiu of other ABV is shown in Table 2. When the ABV is high, the fitting effect of the geometric method is similar to the particle swarm optimization, and the difference of δ value does not exceed 0.1%, better than the least squares method. When the ABV is low, although the value of δ is larger than the particle swarm optimization, it still does not exceed 1%. The difference in values of ε_{r0} , $\varepsilon_{r\infty}$, τ does not exceed 5%. The value of α is very small and has little effect on the value of the Cole-Cole equation. The fitting curve at low ABV is shown in Fig.7. It shows that the parameter fitting effect at low ABV is also better, and the actual data are all distributed near the fitting curve. With the increase of ABV, the fitting effect of the

geometric method based on the Cole-Cole model is getting better, so this method can be well used for Cole-Cole parameter fitting of baijiu.

2.3 ABV Measurement Model and Verification

The ε_{r0} , $\varepsilon_{r\infty}$, τ parameters obtained by the geometric method and their corresponding ABV are linearly fitted. Since the α parameter value hardly changes with the ABV, it is not suitable for the measurement of the ABV of baijiu. The other three parameters change linearly with the increase of ABV, especially the correlation coefficients obtained by the fitting of ε_{r0} and τ parameters. The Cole-Cole parameters of 53% ABV baijiu were calculated by geometric method ($\varepsilon_{r0}=56.47$, $\varepsilon_{r\infty}=2.69$, $\tau=35.24$ ps, $\alpha=0.13$, $\delta=1.07\%$), and the alcohol was analyzed according to this model. The measurement results are shown in Table 3. The error of the prediction result is small, especially the ABV obtained by fitting ε_{r0} , the error is only 1.51%.

Table 2 Three methods of fitting parameter results of other ABV values of baijiu

ABV	Method	ε_{r0}	$\varepsilon_{r\infty}$	α	τ /ps	δ /%
42%	Geometric method	63.17±0.65	1.47±0.43	0.14±0.01	26.59±0.26	0.95
	Least squares method	60.88	2.12	0.11	25.36	0.69
	Particle swarm optimization	60.93	1.81	0.11	25.31	0.68
45%	Geometric method	61.80±0.54	1.58±0.36	0.14±0.01	27.69±0.24	0.98
	Least squares method	59.49	2.28	0.11	26.38	0.66
	Particle swarm optimization	59.54	1.99	0.11	26.35	0.70
50%	Geometric method	57.81±0.53	2.50±0.29	0.13±0.01	31.51±0.34	0.78
	Least Square method	56.02	2.70	0.11	30.00	0.66
	Particle swarm optimization	56.47	2.38	0.12	30.32	0.57
52%	Geometric method	56.80±0.54	2.58±0.293	0.13±0.01	33.01±0.38	0.74
	Least squares method	53.48	2.94	0.10	30.00	0.91
	Particle swarm optimization	55.44	2.47	0.12	31.70	0.57

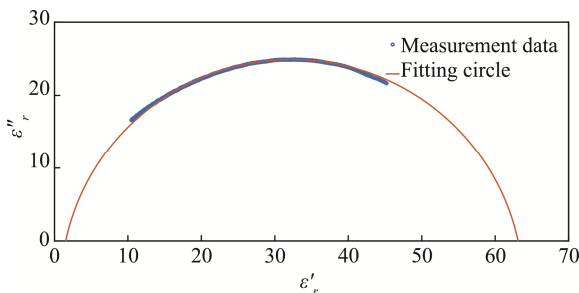


Fig.7 Fitting Cole-Cole curve for complex permittivity of 42% ABV values of baijiu

Table 3 Prediction results and errors of 53% ABV of baijiu

ε_{r0} -ABV		$\varepsilon_{r\infty}$ -ABV		τ -ABV	
Predicted ABV	Relative error	Predicted ABV	Relative error	Predicted ABV	Relative error
52.2%	1.51%	51.5%	2.83%	54.7%	3.2%

3 Discussion

3.1 Selection of Frequency Range

In actual measurement, the frequency range measured by different devices is different. At the same time, in geometric method as the frequency range decreases, the arc length of the complex permittivity data corresponding to the Cole-Cole circle will be shortened. So the fitting accuracy will also decrease. Therefore, the selection of frequency range is discussed. On the basis of 3-20 GHz, the upper and lower limits are shortened by 0.5 GHz each time to verify the effectiveness of the method in a smaller range. The complex permittivity of 53% ABV baijiu was fitted, and the fitting data obtained in different frequency ranges are shown in Table 4. The prediction error is still less than 5% when the frequency range is

reduced to 4-19 GHz, but the prediction error is larger when the frequency range is narrowed again. The method can accurately measure the ABV of baijiu when the frequency range is greater than 4-19 GHz.

3.2 Frequency Point Selection Method

In addition to the isometric axis method, the isometric frequency method is also employed for point acquisition. The distance between two adjacent frequency points is 1/3 of the total number of frequency points (rounded down), take three points to calculate the equation of the Cole-Cole circle, and then calculate the parameter value from the relationship between the Cole-Cole diagram and the model parameters. The ABV of baijiu is selected as 56%, and the result is the average of 50 calculations. The results are $\varepsilon_{r0}=58.96\pm0.53$, $\varepsilon_{r\infty}=1.40\pm0.26$, $\tau=40.05\pm0.45$ ps, $\alpha=0.20\pm0.01$, $\delta=2.51\%$. The circle fitted by the two methods are shown in Fig.8. The δ value calculated by the isometric frequency method is larger, and the fitting effect is worse than the isometric axis method. It can be seen from Fig.8 that the radius error of the Cole-Cole circle fitted by the isometric frequency method is large, resulting in a large parameter fitting error. Since the frequency is selected to be equally spaced, the distribution of the complex permittivity in the complex number domain will become more and more dense with the increase of the frequency. Thus, employing this method for point selection may result in a reduced separation between data points at higher frequencies, leading to significant parameter inaccuracies and a diminished overall fitting quality.

Table 4 Fitting results of baijiu of 53% ABV values in different frequency

Frequency/GHz	3.5-19.5	4-19	4.5-18.5
ε_{r0}	56.46±0.50	57.42±0.62	58.38±0.57
$\varepsilon_{r\infty}$	2.69±0.25	2.39±0.26	2.07±0.20
α	0.13±0.01	0.14±0.01	0.16±0.01
τ /ps	35.12±0.50	36.21±0.69	37.12±0.68
δ	0.85%	1.00%	0.87%
Predicted ABV	52.26%	50.78%	49.29%
Relative error	1.40%	4.20%	7.00%

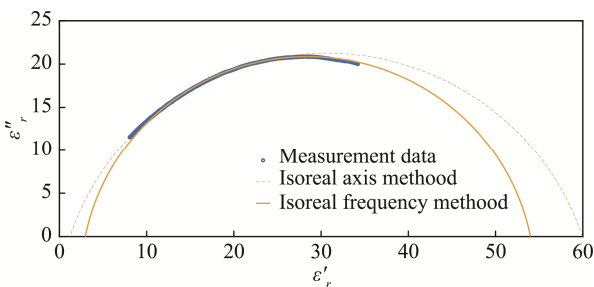


Fig.8 Fitted Cole-Cole curve of the two methods for permittivity of 56% baijiu

3.3 Calculation Method of τ Value

Another calculation method of τ value is also adopted. The τ value is calculated according to the maximum value of the imaginary part of the complex permittivity. First, the frequency point corresponding to the maximum imaginary part is taken out of the measured complex permittivity. Then the calculation equation of the τ value obtained from $\omega\tau=1$.

This method has no effect on the ε_{r0} , $\varepsilon_{r\infty}$, α values. The τ and δ values obtained by calculation are shown in Table 5. It shows that although the τ value is similar to the particle swarm optimization, the δ value calculated by this method is generally larger than the geometric method. When the ABV is 52%, δ reaches the maximum, and the fitting degree is similar when the ABV is 50% and 56%. It can only be used when there are enough frequency points. If there are fewer frequency points, the maximum point of the imaginary part may be far away from the Cole-Cole apex, resulting in a large error. However, when the frequency points are dense, this method can be used for the simple calculation of the τ value and can be obtained before fitting the circle.

Table 5 Results of τ value calculated by $\omega\tau=1$ for baijiu

ABV	42%	45%	50%	52%	53%	56%
τ (ps)	26.90	26.90	31.44	31.44	33.66	36.00
δ	1.04%	2.18%	0.80%	3.34%	1.72%	0.74%

4 Conclusion

A method for the calculation of the complex permittivity parameters of baijiu using the Cole-Cole diagram is proposed. A small fitting error of the complex permittivity has been achieved. The error does not exceed 1%. The calculation is simple, and it can be used for the ABV measurement of baijiu. The fitting of the complex permittivity of 42-56% baijiu over 3-20 GHz has been carried out. The results show that the geometric method and the particle swarm optimization have better fitting than the least squares method. The least squares method has an error with a maximum larger than 1%. This method is used for parameter fitting of baijiu with other ABV, and it is found that this method is also applicable. Finally, a geometric method was used to establish an ABV prediction model, and the 53% baijiu was predicted with an error of 1.51%. This method can be used to measure the ABV of baijiu.

The frequency range is discussed. When the frequency range was narrowed to 4-19 GHz, the error in the methods prediction of ABV was less than 5%. In addition, other methods of taking points and calculating error values are proposed. The fitting result of taking points with equal frequency is poor, and the value of δ reaches 2.51%; the value of error is obtained by calculating the value of τ from the maximum value of the imaginary part. It is between 0.7-3.4%, but the calculation method is simple and can be

used for simple calculation of the τ value when the measurement frequency points are dense. In future research, additional experiments will be conducted to attain a higher level of precision.

The method does not need to preset the value when calculating the Cole-Cole parameter value and has a good fitting of baijiu. It can also be applied to the evaluation of baijiu with other ABV in the future. In addition, the calculation process is simple, and it can provide a more accurate reference for the setting of iterative optimizations such as particle swarm optimization. It can also be used to verify the calculation results of other optimizations.

Author Contributions:

Here is a breakdown of the specific contributions of each author based on the suggested roles:

[Yu Haoyan]: Data curation; Formal analysis; Writing - original draft; Writing - review & editing.

[Jin Qi]: Investigation; Methodology; Validation; Resources; Writing - review & editing.

[Meng Zhaozong]: Resources; Writing - review & editing.

[Li Zhen]: Conceptualization; Writing - review & editing.

Authors have identified roles that apply to their contributions realistically and accurately, ensuring a fair and transparent acknowledgment of each member's involvement in the research.

Funding Information:

This work was financially supported by the Postgraduate Research & Practice Innovation Program of Jiangsu Province (Grant No. SJCX23_0099)

Data Availability:

All data supporting the results of this study are included in the manuscript and are available upon request.

Conflict of Interest:

The authors declare no competing interests.

Dates:

Received 18 October 2023; Accepted 11 January 2024; Published online 31 March 2024

References

- [1] Zheng J, He L. (2014). Surface-Enhanced Raman Spectroscopy for the Chemical Analysis of Food. *Comprehensive Reviews in Food Science and Food Safety*, 13(3), pp.317-328.
- [2] Chen D, Tan Z, Huang Z, et al. (2019). Detection of lethal fake liquors using digitally labelled gas-phase Fourier transform infrared spectroscopy. *Spectroscopy Letters*, 52(3-4), pp.204-210.
- [3] Bordiga M, Rinaldi M, Locatelli M, et al. (2013). Characterization of Muscat wines aroma evolution using comprehensive gas chromatography followed by a post-analytic approach to 2D contour plots comparison. *Food Chemistry*, 140(1-2), pp.57-67.
- [4] Seo S, Kim E, Park S, et al. (2020). GC/MS-based metabolomics study to investigate differential metabolites between ale and lager beers. *Food Bioscience*, 36, pp.100671.
- [5] Coelho E, Lemos M, Genisheva Z, et al. (2020). Validation of a LLME/GC-MS Methodology for Quantification of Volatile Compounds in Fermented Beverages. *Molecules*, 25(3), pp.621
- [6] Del Carlo M, Pepe A, Sacchetti G, et al. (2008). Determination of phthalate esters in wine using solid-phase extraction and gas chromatography–mass spectrometry. *Food Chemistry*, 111(3), pp.771-777.
- [7] Jiang H, Mei C, Li K, et al. (2018). Monitoring alcohol concentration and residual glucose in solid state fermentation of ethanol using FT-NIR spectroscopy and L1-PLS regression. *Spectrochimica Acta Part A: Molecular and Biomolecular Spectroscopy*, 204, pp.73-80.
- [8] Hu L, Yin C, Ma S, et al. (2018). Rapid detection of three quality parameters and classification of wine based on Vis-NIR spectroscopy with wavelength selection by ACO and CARS algorithms. *Spectrochimica Acta Part A: Molecular and Biomolecular Spectroscopy*, 205, pp.574-581.
- [9] Li Z, Haigh A, Wang P, et al. (2021). Characterisation and analysis of alcohol in baijiu with a microwave cavity resonator. *LWT-Food Science and Technology*, 141, pp.110849.
- [10] Li Z, Meng Z, Haigh A, et al. (2021). Characterisation of water in honey using a microwave cylindrical cavity resonator sensor. *Journal of Food Engineering*, 292, pp.110373.
- [11] Li Z, Haigh A, Soutis C, et al. (2017). Evaluation of water content in honey using microwave transmission line technique. *Journal of food Engineering*, 215, pp.113-125.
- [12] Guo W, Fang L, Liu D, et al. (2015). Determination of soluble solids content and firmness of pears during ripening by using dielectric spectroscopy. *Computers and Electronics in Agriculture*, 117, pp.226-233.
- [13] Soltani M, Alimardani R, Omid M. (2011). Evaluating banana ripening status from measuring dielectric properties. *Journal of Food Engineering*, 105(4), pp.625-631.
- [14] Zhao K, Liu Y, Zhang Q. (2019). Dielectric behavior of adulterated milk with urea and water. *Journal of Molecular Liquids*, 273, pp.37-44.
- [15] Guo W, Zhu X, Liu H, et al. (2010). Effects of milk concentration and freshness on microwave dielectric

- properties. *Journal of Food Engineering*, 99(3), pp.344-350.
- [16] Castro-Giraldez M, Toldra F, Fito P. (2011). Low frequency dielectric measurements to assess post-mortem ageing of pork meat. *LWT - Food Science and Technology*, 44(6), pp.1465-1472.
- [17] Perez-Esteve E, Fuentes A, Grau R, et al. (2014). Use of impedance spectroscopy for predicting freshness of sea bream (*Sparus aurata*). *Food Control*, 35(1), pp.360-365.
- [18] Guo C, Xin L, Dong Y, et al. (2018). Dielectric Properties of Yogurt for Online Monitoring of Fermentation Process. *Food and Bioprocess Technology*, 11(5), pp.1096-1100.
- [19] Yang J, Zhao K S, He Y J. (2016). Quality evaluation of frying oil deterioration by dielectric spectroscopy. *Journal of Food Engineering*, 180, pp.69-76.
- [20] Li Z, Wang N, Raghavan G S V, et al. (2011). Volatiles Evaluation and Dielectric Properties Measurements of Chinese Spirits for Quality Assessment. *Food and Bioprocess Technology*, 4(2), pp.247-253.
- [21] Miura N, Yagihara S, Mashimo S. (2003). Microwave Dielectric Properties of Solid and Liquid Foods Investigated by Time-domain Reflectometry. *Journal of food science*, 68(4), pp.1396-1403.
- Bohigas X, Tejada J. (2010). Dielectric characterization of alcoholic beverages and solutions of ethanol in water under microwave radiation in the 1–20 GHz range. *Food Research International*, 43(6), pp.1607-1613.
- [22] Li Z, Haigh A, Wang P, et al. (2021). Dielectric spectroscopy of Baijiu over 2–20 GHz using an open-ended coaxial probe. *Journal of Food Science*, 86(6), pp.2513-2524.
- [23] Mason P R, Hasted J B, Moore L. (1974). The use of statistical theory in fitting equations to dielectric dispersion data. *Advances in Molecular Relaxation Processes*, 6(3), pp.217-232